


CME deflections due to magnetic forces from the Sun and Kepler-63

F. Menezes¹ , Y. Netto^{1,2}, C. Kay³, M. Opher⁴ and A. Valio¹

¹Universidade Presbiteriana Mackenzie, CRAAM, São Paulo, Brazil
email: menezes.astroph@gmail.com

²Osservatorio Astrofisico Di Catania, Catania, Italy

³NASA, Goddard Space Flight Center, Greenbelt, USA

⁴Boston University, Department Of Astronomy, Boston, USA

Abstract. The stellar magnetic field is the driver of activity in the star and can trigger energetic flares, CMEs and ionized wind. These phenomena, specially CMEs, may have an important impact on the magnetosphere and atmosphere of the orbiting planets. To predict whether a CME will impact a planet, the effects of the background on the CME's trajectory must be taken into account. We used the MHD code ForeCAT – a model for CME deflection due to magnetic forces – to perform numerical simulations of CMEs being launched from both the Sun and Kepler-63, which is a young, solar-like star with high activity. Comparing results from Kepler-63 and the Sun gives us a panorama of the distinct activity level and star-planet interactions of these systems due to the difference of stellar ages and star-planet distances.

Keywords. Sun: coronal mass ejections (CMEs), stars: activity, stars: magnetic fields, stars: spots, MHD

1. Introduction

The average surface magnetic field of the Sun is about 1 G, however in some regions the field may reach values up to several hundred gauss in photospheric features such as sunspots and faculae. These features are observable proxies of solar magnetic activity, providing a window to the unseen internal dynamo and acting as tracers of magnetic topology. Sunspots and faculae are the surface emanations of internal magnetic fields caught in turbulent flows that eventually become areas of amplified magnetic fields when erupting through the photosphere. The occurrence of these features has an 11-year modulation. This is known as the solar activity cycle, in which the magnetic field of the Sun reverses its polarity forming a magnetic cycle of 22 years. During solar maxima, energetic events like coronal mass ejections (CME), increased solar wind, and flares are more common.

The stellar activity is related to the age of the star. The Sun for instance with an age of 4.6 billion years is considered just a mildly active star, while Kepler-96 – an active solar-type star of 2.3 billion years – is a very active star presenting super flares of 1.8^{35} ergs in its light curves (Estrela & Valio 2018). Stars interact with their orbiting planets through their magnetic field and energetic events, specially CMEs that may impact on the magnetosphere and atmosphere of these planets.

Despite being at 1 AU away from the Sun, on Earth CMEs can cause geomagnetic storms and affect the communication systems, power lines, satellites orbits, etc. Observations from Mars have shown that CMEs can have a significant impact on the

atmosphere and the long-term atmospheric evolution of the planet, suggesting that space weather can affect the habitability of a planet through atmospheric losses (Jakosky 2015). Close-in planets – such as hot Jupiters around solar-like stars and planets in the habitable zone of active M dwarfs – may experience more extreme space weather than on Earth, including frequent CME impacts leading to atmospheric erosion and leaving the surface exposed to extreme radiation from flare activity (Kay *et al.* 2016).

It is very important to be able to predict CMEs trajectories since that is what determines if a CME will hit a planet and cause important impact in space weather. Our goals are to simulate CMEs trajectories and deflections which are subject to the magnetic forces, being launched from the Sun and Kepler-63 – a young, highly active, solar-like star with ~ 210 Myr, $0.984 M_{\odot}$, $0.901 R_{\odot}$ and a 5.4-day rotation period (Sanchis-Ojeda *et al.* 2013) – and then compare results from both stars in order to have a panorama of the distinct activity level and star-planet interactions of these systems due to the difference of stellar ages and star-planet distances.

2. Numerical simulations

To run the simulations we used the ForeCAT (Forecasting a CME's Altered Trajectory, Kay *et al.* 2013), an MHD code created to simulate CME deflections and rotations due to magnetic forces which are the magnetic pressure gradients and the magnetic tension. It divides the propagation of the CME in three parts: gradual rise, impulsive acceleration, and propagation. Also, it includes CME expansion and the effects of drag on the CME's deflection. The CME simulations are initiated by setting the launch site on the stellar surface (latitude and longitude), tilt (measured clockwise with respect to the equatorial plane), shape parameters, and other properties of the CME such as mass, final propagation speed, initial radius, and initial magnetic strength (Kay *et al.* 2015). The shape parameters A , B and C describe an elliptical toroidal CME. A is defined as the axis in the direction of the nose of the CME (the point on the surface of the torus with greatest radial distance) and C is the initial distance of the nose from the star surface. The radius B describes the cross section of the torus.

This code uses the Potential Field Source Surface (PFSS) model to calculate the stellar background magnetic field, which assumes that the magnetic field can be described as current-free and becomes entirely radial above the source surface (Kay *et al.* 2015). The source surface is typically taken to be $2.5 R_{\star}$ for PFSS models of the Sun. The smaller the radius, the greater the influence of the active regions and the smaller the influence of the coronal holes on the source surface magnetogram, and vice versa. Therefore, we performed simulations with source surfaces of 1.05 and $2.5 R_{\star}$ to explore the influence of the magnetic density flux in the spots of both stars.

To calculate the stellar background magnetic field, the input parameter is a photospheric magnetogram, which in the case of the Sun a magnetogram from 1 solar rotation (CR2203), however such data is not available for Kepler-63. The only information on the photosphere of the star from transits light curves from Kepler Space Telescope, were the starspots mapped by Netto & Valio (2019). These starspots were mapped using the model from Silva (2003), which allows determining the physical characteristics of the spots, such as size, temperature, and location. Also, Kepler-63 was chosen because it harbors a hot Jupiter (Kepler-63 b) orbiting in an almost polar orbit, which allows mapping starspots at different latitudes. Figure 1 shows all mapped spots.

Then, to obtain a magnetogram we used the relation between spots intensity and magnetic field determined from 32,000 sunspots (Valio *et al.* 2019):

$$B = (4848 \pm 15) - (4008 \pm 20) \times I, \quad (2.1)$$

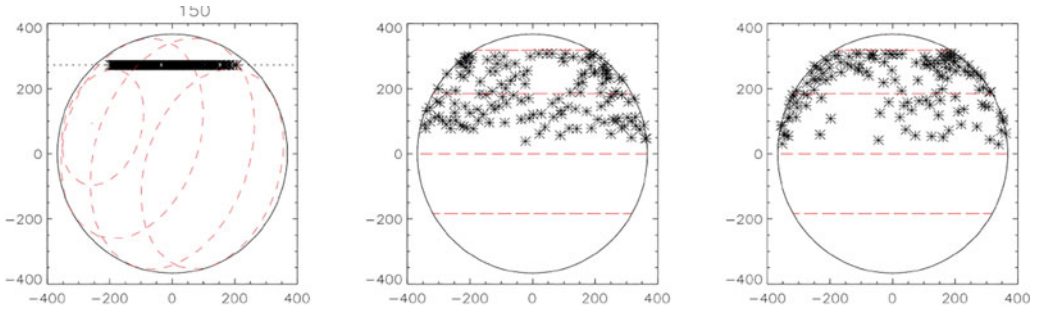


Figure 1. Kepler-63's spots. *Left panel:* spots over-plotted in a referential frame as seen from Earth. *Right panel:* all mapped spots in a frame rotating with the star

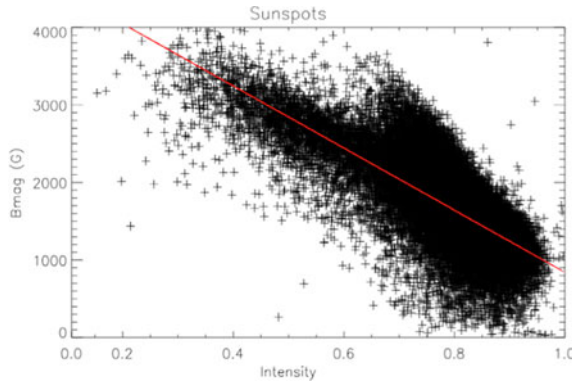


Figure 2. Sunspot intensity vs sunspot magnetic density flux. The red line is the linear equation fitted (Eq. 2.1)

where B is the maximum magnetic density flux and I is the spot intensity (normalized to the star intensity at the center of the disk). To obtain magnetic field intensities of spots on Kepler-63, we used the values of spot intensities from the fit of the light curves variations observed on the 88th transit of the planet. The intensities of the spots – 0.398, 0.416 and 0.486 (from South to North in the left panel in Figure 3) – yield respectively magnetic density flux values of 3258, 3186 and 2906 G (or Mx/cm²). The magnetogram was created by inserting the magnetic flux in a dipole spread within the starspot area (right panel in Figure 3). Also, for the background magnetic field, we used the CR2203 magnetogram without the large active regions, and multiplied by three, since the active regions in Kepler-63 were three time stronger than the Sun's.

For both CME simulations we set initial position at $1.1R_*$, so the shape parameter C was $0.1R_*$ and the ratios A/C and B/C were 1.0 and 0.2, respectively. The final position was set at $10R_*$, initial latitude at 16.5° , initial longitude at 316.8° , initial tilt of -35° and masses equal to 10^{15} g.

3. Results and conclusions

We performed a total of 4 simulations – 2 for the Sun and 2 for Kepler-63 – with the source surface taken at 2 different values – 1.05 and $2.5 R_*$. Figure 4 shows the CME simulations output parameters – tilt, latitude, longitude and radial velocity over the distance from the star. The tilt of the deflection is larger in the case of the CME launched from Kepler-63 (57°) than that of the Sun (45°). Simulations from Kepler-63 with the source surface at $1.05 R_*$ presented all output parameters, except radial velocity,

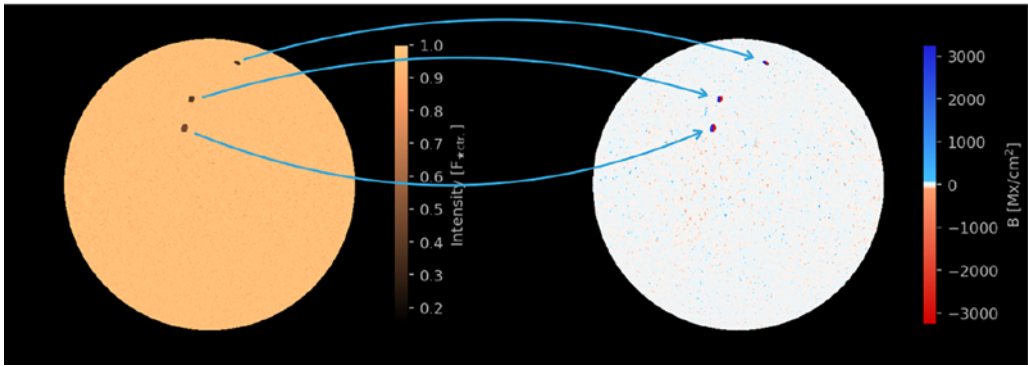


Figure 3. Kepler-63's mapped starspots from the transit no. 88. *Left panel:* relative intensity color scale *Right panel:* magnetic density flux color scale.

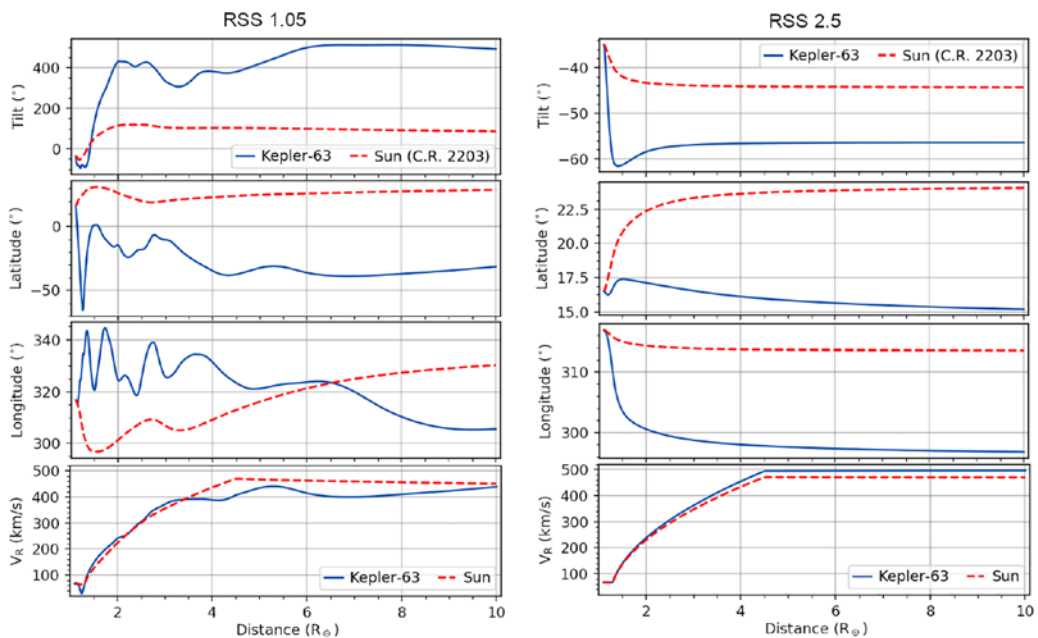


Figure 4. CME simulations outputs. Tilt, latitude, longitude and radial velocity over the distance from the star. The blue solid lines represents the Kepler-63 and the red dashed lines represents the Sun.

to have significant variations over the distance up to $\sim 3R_*$, and for both source surface values, the output parameters from Kepler-63 – tilt, latitude and longitude – are more intense than the simulations from the Sun. Despite the initial discrepancy, the velocities of the sun and Kepler-63 CME approximate each other at 10 radii.

With the source surface taken at lower heights, such as $1.05 R_*$, the influence of the active regions are stronger and the background magnetic field presents an intricate configuration, causing the trajectory and rotation of the CME to present more variation. The background magnetic field tends to approximate to the heliospheric current sheet with the source surface taken at $2.5 R_*$, but due to a 3-time stronger magnetic field, the CMEs from Kepler-63 undergo higher deflections and rotation.

References

- Estrela, R. & Valio, A. 2018, *Astrobiology*, 18, 1414
- Jakosky, B. M. 2015, *Science*, 350, 643
- Kay, C., Opher, M., & Evans, R. M. 2013, *Astrophys. J.*, 775, 5
- Kay, C., Opher, M., & Evans, R. M. 2015, *Astrophys. J.*, 805, 168
- Kay, C., Opher, M., & Kornbleuth, M. 2016, *Astrophys. J.*, 826, 195
- Netto, Y. & Valio, A. 2019, *A&A* (accepted)
- Sanchis-Ojeda, R., Winn, J. N., Marcy, G. W., *et al.* 2013, *Astrophys. J.*, 775, 54
- Silva, A. V. R. 2003, *Astrophys. J. Lett.*, 585, L147
- Valio, A., Spagiari, E., Marengoni, M., & Selhorst, C. 2019, Manuscript in preparation